



Contents lists available at ScienceDirect

Applied Clay Science

journal homepage: [www.elsevier.com/locate/clay](http://www.elsevier.com/locate/clay)

Research Paper

## Determining the size distribution-defined aspect ratio of platy particles

 Daniel Gantenbein <sup>a,b,\*</sup>, Joachim Schoelkopf <sup>a</sup>, G. Peter Matthews <sup>b</sup>, Patrick A.C. Gane <sup>a,c</sup>
<sup>a</sup> Omya Development AG, Baslerstrasse 42, CH-4665 Oftringen, Switzerland

<sup>b</sup> Environmental and Fluid Modelling Group, University of Plymouth, Plymouth PL4 8AA, UK

<sup>c</sup> Department of Forest Products Technology, Aalto University, Espoo, FI-00076 Aalto, Finland

### ARTICLE INFO

#### Article history:

Received 26 July 2010

Received in revised form 15 April 2011

Accepted 20 April 2011

Available online xxx

#### Keywords:

Aspect ratio

Talc

Laponite

Laser light scattering

Sedimentation

Specific surface area

### ABSTRACT

Mineral particles are used in many industrial applications as fillers, in coatings, as ad- and absorbers or in catalysis. In these manifold fields the particle size and shape control the final performance and properties of the minerals. Much has been published using different techniques to describe the aspect ratio of platy particles. This study describes a simple method to calculate aspect ratios for platy particles based on particle size data and specific surface area determined by nitrogen adsorption, exemplified with three different talc grades which vary in their amount of specific surface area and geological origin, as well as with one nano-sized synthetic Laponite (Laponite® RD) to illustrate the sensitivity to input parameters and their physical interpretation. The contrast between mass/volume and number probability distribution of particle size is discussed and illustrated.

© 2011 Elsevier B.V. All rights reserved.

### 1. Introduction

Mineral particles are used as fillers in a range of applications, including paper, decorative and functional coatings, plastics and ceramics (Baudet et al., 1993; Ferrage et al., 2003; Gane, 2001; Gane et al., 1995; Lohmander, 2000; Murray and Kogel, 2005; Naito et al., 1998). Frequently, the morphology of the particles constituting the mineral within a desired particle size distribution can be a key factor in determining the functionality of the end use. Mineral particles like talc are found in paper coatings and as paper fillers in the bulk of the fibrous sheet. They are also applied as filtration aids or as a component in fixed bed reactors (Aris, 1957; Casal et al., 1985), and found in cosmetic products (Papirer et al., 1992). In all these application fields, the particle shape is of great importance. For example, in paper, platy talc or acicular aragonite provide for coating coverage and internal bulk, respectively. Minerals may also expose different surface properties, depending on the orientation of the particulate in respect to its morphology. The ratio of anisometric surfaces may control properties such as wettability to certain liquids, which can affect mineral processing and end-use function or the rheological behaviour of a particle suspension (Gane, 1997; Gane et al., 1997; Gane and Coggon, 1987; Gane and Watters, 1989; Kroon et al., 1998; Morris et al., 1965; Mouchid et al., 1995;

Mouchid and Levitz, 1998). A typical example was given by Yekeler et al. (2004) and Yildirim (2001) in respect to the specific adsorption potential of a mineral in relation to its surface differential properties. Similarly, minerals used as catalysts owe their functionality to the exposure of the required reactive surface. Thus, for simple planar and longitudinal geometries, it is crucial for assessing particle-related performance to ascertain a representation of the aspect ratio (Li et al., 2002). Aspect ratio expresses the relative abundance of the two characteristic surfaces of platy particles, and is defined generally as the ratio of the major axis dimension to that of the minor dimension. In the case of platy particles this is given by the ratio of the major diameter of the planar platelet to its laminar thickness. The thickness of a platy particle may for some minerals be in the region of a few nanometres, having thus an effectively very high localised curvature and thus a very high surface free energy.

Different techniques to measure or determine aspect ratios were reported in the literature. A vast number of studies (Baudet et al., 1993; Jennings and Parslow, 1988; Lohmander, 2000; Pabst et al., 2000, 2001, 2006a,b, 2007; Pabst and Berthold, 2007; Slepetyts and Cleland, 1993) described how laser ensemble diffraction and single particle light scattering (static and dynamic) offer an opportunity to measure aspect ratios. The same authors also referred to gravitational sedimentation, which is effective for particles greater than the suspension-maintained Brownian motion limit. Many of the above quoted methods had their basis in the work published by Jennings and Parslow (1988). They derived the transformation of an equivalent spherical diameter (esd), as manifest by the various sizing techniques,

\* Corresponding author at: Omya Development AG, Baslerstrasse 42, CH-4665 Oftringen, Switzerland. Tel.: +41 62 789 23 30; fax: +41 62 789 24 00.

E-mail address: [daniel.gantenbein@omya.com](mailto:daniel.gantenbein@omya.com) (D. Gantenbein).

**Table 1**  
Formulae to calculate the disc diameter  $d$  based on the esd ( $d_s$ ,  $d_a$ ,  $d_v$  and  $d_T$ ) response from the corresponding particle sizing method.

Particle sizing method	
Sedimentation (Sedigraph®)	$d_s = d\sqrt{\frac{3}{2\rho}} \tan^{-1}(\rho)$
Laser light scattering/Projected area (Fraunhofer)	$d_a = d\sqrt{\frac{1}{2} + \frac{1}{\rho}}$
Laser light scattering/Particle volume (Mie theory)	$d_v = d\sqrt{\frac{3}{2\rho}}$
Photon correlation spectroscopy/Translational diffusion	$d_T = \frac{d}{\tan^{-1}(\rho)}$

into the major particle dimension, i.e. platelet diameter for the cases studied here (Table 1).

$\rho$	aspect ratio
$d_s$	particle diameter based on sedimentation
$d_a$	particle diameter based on projected area/static laser light scattering with Fraunhofer optics
$d_v$	particle diameter based on particle volume/static laser light scattering with Mie theory
$d_T$	particle diameter based on translatory diffusion/photon correlation spectroscopy (PCS)

By combining two of the particle size measurement methods, e.g. sedimentation and projected area, they extracted an aspect ratio defined purely at one given particle size (Eq. (1)). Eq. (1) is derived for oblate spheroids, and can, thus, be adopted to calculate the aspect ratio of platy minerals, as in the limit of extremely high aspect ratio, the formula reduces to that for a circular disc (Eq. (2)).

$$\frac{d_s}{d_a} = \frac{2 \cdot \rho \cdot \tan^{-1}(\sqrt{\rho^2 - 1})}{\rho \cdot \sqrt{\rho^2 - 1} + \ln(\rho + \sqrt{\rho^2 - 1})} \quad (1)$$

$$\frac{d_s}{d_a} = \frac{3 \cdot \tan^{-1}(\rho)}{(\rho + 2)} \quad (2)$$

A similar approach was presented by Pabst and Berthold (2007) (Eq. (3)). However, the model of Pabst and Berthold (2007) overestimates the aspect ratio. In the case of high aspect ratios  $\tan^{-1}(\rho)$  becomes  $\pi/2$  and so Eq. (2) can be solved for  $\rho$  (Eq. (4)) which shows that the approximation of Pabst and Berthold (2007) differs from the Jennings and Parslow (1988) model by an addition of 2.

$$\rho = \frac{3\pi}{2} \cdot \left(\frac{d_a}{d_s}\right)^2 \quad (3)$$

$$\rho + 2 = \frac{3\pi}{2} \cdot \left(\frac{d_a}{d_s}\right)^2 \quad (4)$$

The turbidity of colloidal kaolinite particles as a function of random or shear flow orientation was used to extract shape information as presented by Champion et al. (1979). Champion et al. (1978) also published a magneto-optical method to determine the particle shape via the particle area (permanent magnetic moment) and the particle volume (magnetic susceptibility anisotropy). Another possibility identified, was to use scanning and transmission electron microscopy together with image analysis, employing such techniques as particle shadowing (Conley, 1966; Morris et al., 1965; Podczek, 1997; Yekeler et al., 2004). Further literature exemplified methods including FTIR measurements made from deuterium structure-exchanged particles (Ferrage et al., 2003) or calorimetric measurements (Groszek and Partyka, 1993; Yildirim, 2001). X-ray

diffraction (XRD) was also regularly used to describe surface texture of compacted powders, and particle orientation, but the technique also delivered information related rather to crystallite size than to particle size or relative anisotropy. The correlation of crystallite size and peak width was first described by Scherrer (1918). Also small angle X-ray scattering measurements were reported by some authors to estimate the aspect ratio of disc-like particles like Laponite (Kroon et al., 1996, 1998).

This study focused on the Hohenberger model (Hohenberger, 2001). The advantage of this model is the fact that it has two independent parameters, namely the specific surface area and the particle size. Both parameter determination methods are readily available and are routinely measured in the analysis of mineral particles. The model assumed a disc-like geometry to represent the platy particles and calculated the aspect ratio from the measured specific surface area by BET (Brunauer et al., 1938) and by a necessarily well-defined particle size measurement. Despite the reasonable results usually received by the Hohenberger approach (Hohenberger, 2001), some significantly false assumptions in respect to parameter input were frequently presented in the literature. This paper set out to clarify these issues, improved the application and definition of the model and further applied it by way of illustration for two platy particles (talc and Laponite (Laponite® RD)), which represent materials having typical particle size distributions to be found in many industrially relevant applications. Additionally, by contrasting talc particles with Laponite particles swelling in water, the sensitivity to the input parameters in respect to their physical interpretation was illustrated.

### 1.1. Particle size definitions

For a general overview of the theoretical and experimental aspects of particle size measurements the reader is referred to the book of Allen (1997) as also the informative summary of the methods published by Schoelkopf et al. (2008). Nevertheless, it is important to mention the basis of frequently used particle size analysis techniques. Particle diffraction of a light beam relates to the projected area of a particle, the scattering cross-section if Fraunhofer optics are used (Jennings, 1993). Alternatively, the Mie theory applied to the angular scattering intensity distribution (Mie, 1908) expresses the particle optical path length, and hence particle volume under random orientation (Jennings, 1993; Schmidt, 2000). In this study, a Malvern Mastersizer 2000 was used for both the Fraunhofer- and Mie-theory-based measurements, entering the refractive indices and specific wavelength light absorption constants for each mineral. The drawback of both methods is that laser scattering as a technique only detects the particles according to the respective theory limitations. Concentration is not known generally when such measurements are made, and so distributions, normalised to the observed particles only, tend to ignore ultra fine and ultra coarse particles. The normalisation is then, per force, restricted to within the assumed observed range.

By way of contrast, dynamic light scattering (DLS), based on photon correlation spectroscopy (PCS), expresses an equivalent Stokes–Einstein translational diffusion diameter including the mineral core and any associated layer of adsorbate, such as dispersant and water. In this method, the ensemble distributed translatory diffusion coefficient is the influential particle parameter. For this technique, a Malvern Zetasizer Nano ZS<sup>1</sup> was used.

Sedigraph<sup>®2</sup> measures the cumulative mass distribution over the defined range of particle size (= volume at known density), and is expressed as an equivalent Stokes settling diameter. Normalisation

<sup>1</sup> Malvern Instruments Ltd., Enigma Business Park, Grovewood Road, Malvern, Worcestershire WR14 1XZ, United Kingdom.

<sup>2</sup> Micromeritics NV/SA, Eugene Plaskyalaan 140, 1030 Brussels, Belgium.

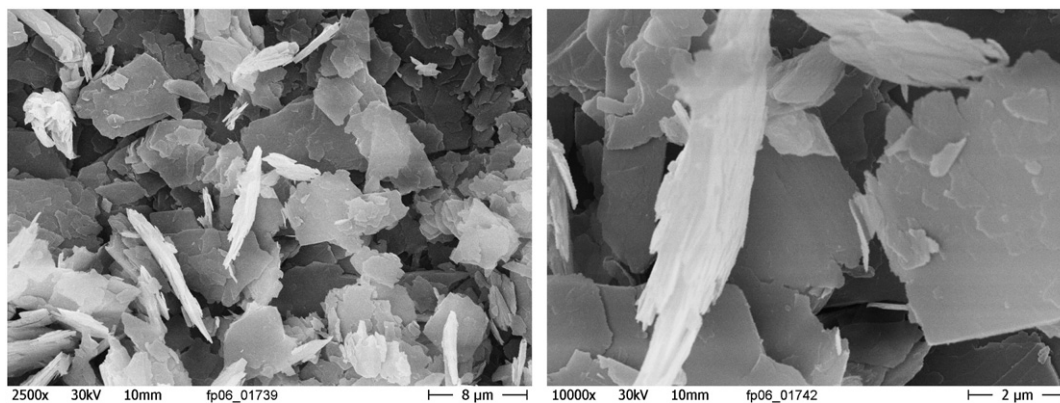


Fig. 1. SEM pictures of the Finnish talc.

considers the whole mass range that then falls within the radiation decay of the Beer–Lambert size (path length) used to determine particle concentration,  $C(h, \tau)$ , at height,  $h$ , after settling time,  $\tau$ .

### 1.2. Conversion of mass to number distribution (and vice versa)

To describe the particle occurrence statistically, it is necessary to convert from the commonly used mass (volume) distribution to number distribution.

Sedimentation requires a shape model (sphere as easiest assumption) and density to express the number of particles in a given size/mass range for comparison with light scattering, whereas light scattering requires the analysis to be applied the other way round for comparison with sedimentation. Light scattering starts with a given spherical model from the number of particles having a given scattering cross-section/volume/-diffusion diameter, after which these values are converted using an assumed density to give a volume distribution. The relevance of either the volume/mass defined size or the number based most common particle, depends on the final application in question. The existence of nanoparticles, for example, is best described by particle number distribution and not by mass, whereas the effect per unit coat mass in a coating layer or the effect per pair-wise interaction in catalysis are best described by volume or mass distribution, respectively.

### 1.3. Aspect ratio ( $\rho$ )

#### 1.3.1. Definition

This study focussed on platy particles (talc and Laponite), while in a second publication the model is further expanded for rod-like particles (Gantenbein et al., in press). In the case of platelets, the

aspect ratio  $\rho$  is defined, via a disc approximation to the platelet shape, by dividing the major diameter  $d$  by the thickness  $t$  (Eq. (5)).

$$\rho = \frac{d}{t} \quad (5)$$

Although the model assumed circular discs to represent irregular shaped platelets (flakes), this was, nevertheless, generally considered reasonable (Jennings and Parslow, 1988; Pabst and Berthold, 2007).

#### 1.3.2. The Hohenberger model

According to Hohenberger (2001) the representative aspect ratio of the platy particles like talc or kaolin can be calculated by

$$\rho = \frac{\varepsilon_{\text{BET}} \cdot d_{50} \cdot e^{-\ln^2\left(\frac{d_{84}}{d_{50}}\right)} \cdot \delta_F - 4}{2} \quad (6)$$

in which the measured variables were defined as,

$\varepsilon_{\text{BET}}$	specific surface area by nitrogen adsorption (BET)
$d_{84}$	particle size at 84% of the sample having less than this size
$d_{50}$	particle size at 50% of the sample having less than this size
$\delta_F$	density of the filler/mineral.

#### 1.3.3. Derivation and development of the model

Hohenberger (2001) did not define the particle size measurement method. Following the manuscript, sieving for coarse particles or

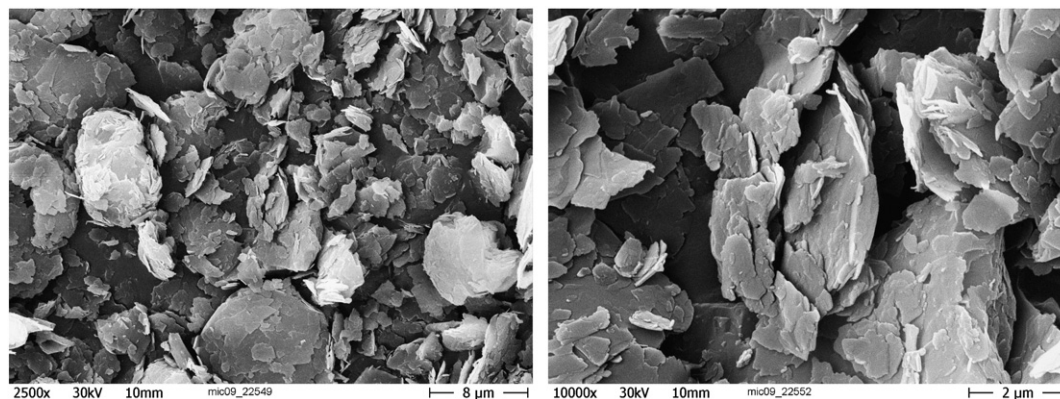


Fig. 2. SEM pictures of the Australian talc.

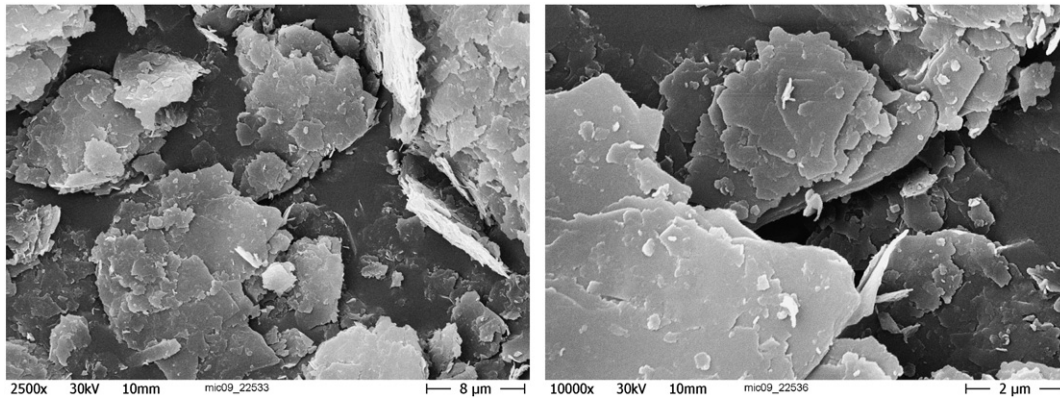


Fig. 3. SEM pictures of the high surface area talc.

sedimentation for fine particles could be the methods of choice for particle size analysis. Applying Stokes' law for particle size measurement results in an equivalent spherical diameter (esd), which is not corresponding to the disc diameter  $d$ , needed for the rigorous application of Hohenberger's equation, Eq. (6) (Jennings and Parslow, 1988; Pabst et al., 2001). Furthermore, it is very unclear from the literature (Hohenberger, 2001) whether the cumulative particle size curve should be used in number, volume or mass (for which the latter two are the same if a constant density applies for all particles in the system).

The aspect ratio  $\rho$  of a circular disc-like particle is given in Eq. (5). The surface area  $s$  of one particle is given by

$$s = 2 \left( \frac{\pi \cdot d^2}{4} \right) + \pi \cdot d \cdot t \quad (7)$$

and so, we can express the aspect ratio  $\rho$  as

$$\frac{1}{\rho} = \frac{s}{\pi \cdot d^2} - \frac{1}{2}. \quad (8)$$

The specific surface area (ssa)  $\varepsilon$  for a single particle is defined as

$$\varepsilon = \frac{s}{m} \quad (9)$$

where  $m$  is the mass of the particle having the surface area  $s$ . If the density of the material is  $\delta$ , then

$$\varepsilon = \frac{s}{\left( \frac{\pi \cdot d^2 \cdot t}{4} \right) \delta} \quad (10)$$

which gives

$$s = \varepsilon \left( \frac{\pi \cdot d^2 \cdot t}{4} \right) \delta \quad (11)$$

applying to Eq. (8), provides

$$\frac{1}{\rho} = \frac{\varepsilon \left( \frac{\pi \cdot d^2 \cdot t}{4} \right) \delta}{\pi \cdot d^2} - \frac{1}{2} = \frac{\varepsilon \cdot \delta \cdot t - 2}{4} \quad (12)$$

and

$$\rho = \frac{4}{\varepsilon \cdot \delta \cdot t - 2}. \quad (13)$$

By eliminating the particle thickness  $t$  by substituting with the expression for  $\rho$  from Eq. (5), we obtain

$$\rho = \frac{4}{\frac{\varepsilon \cdot \delta \cdot d}{\rho} - 2} \quad (14)$$

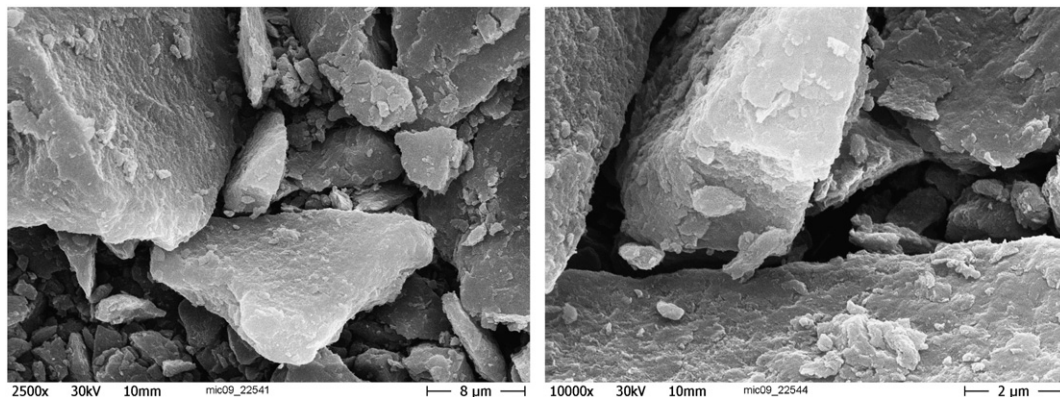


Fig. 4. SEM picture of Laponite.

**Table 2**  
Specific surface area determined by nitrogen adsorption and density of the investigated minerals.

	FT	AT	HSA	Laponite
Specific surface area (BET)/m <sup>2</sup> g <sup>-1</sup>	9	19	45	330
Density/kgm <sup>-3</sup>	2750	2750	2750	2570

such that

$$\rho = \frac{\varepsilon \cdot \delta \cdot d - 4}{2} \quad (15)$$

With the knowledge of the specific surface area determined by the BET method (Brunauer et al., 1938),  $\varepsilon_{\text{BET}}$ , expressed in m<sup>2</sup>kg<sup>-1</sup>, the aspect ratio can be written as

$$\rho = \frac{\varepsilon_{\text{BET}} \cdot \delta_{\text{M}} \cdot d - 4}{2} \quad (16)$$

$\varepsilon_{\text{BET}}$  specific surface area by nitrogen adsorption (BET) in m<sup>2</sup>kg<sup>-1</sup>  
 $\delta_{\text{M}}$  mineral particulate density in kgm<sup>-3</sup>.

In most cases, particle size distributions were described statistically by using the log-normal distribution (Randall, 1989). In a log-normal distribution the particle with the most occurrence probability is given by the mode value,

$$\bar{d}_N = e^{\mu - \sigma^2} \quad (17)$$

where  $\mu$  and  $\sigma$  are the natural log geometric mean and natural log standard deviation respectively, such that the median (midpoint or 50% value) is expressed by

$$d_{N50} = e^{\mu} \quad (18)$$

The geometric standard deviation  $\sigma$  of a log-normal distribution is determined either by dividing the number median particle diameter (which is the particle size where 50% of the particles are finer than this size) by the particle size at 15.78% or by dividing the particle size at 84.13% by the number median particle diameter (Aitchison and Brown, 1957).

$$\sigma = \frac{d_{N50}}{d_{N15.78}} = \frac{d_{N84.13}}{d_{N50}} \quad (19)$$

**Table 3**  
 $d_{N50}$  and  $d_{N84}$  based on a fitted logarithmic cumulative distribution performed with TableCurve 2D.

Method		FT	AT	HSA
PCS	$d_{N50}/\text{nm}$	480	390	450
	$d_{N84}/\text{nm}$	570	510	620
SLLS/Fraunhofer	$d_{N50}/\text{nm}$	500	550	530
	$d_{N84}/\text{nm}$	920	1170	830
SLLS/Mie	$d_{N50}/\text{nm}$	2400	2030	1930
	$d_{N84}/\text{nm}$	4040	3420	3600
Sedigraph®	$d_{N50}/\text{nm}$	340	280	270
	$d_{N84}/\text{nm}$	600	450	400

Thus, dealing with a number distribution, and not the commonly used mass (volume) percent, results in

$$\bar{d}_N = d_{N50} \cdot e^{-\ln^2\left(\frac{d_{N84.13}}{d_{N50}}\right)} \quad (20)$$

Combining Eq. (16) with Eq. (20), leads to Eq. (21). This equation is very similar to the one proposed by Hohenberger (2001).

$$\rho = \frac{\varepsilon_{\text{BET}} \cdot d_{N50} \cdot e^{-\ln^2\left(\frac{d_{N84}}{d_{N50}}\right)} \cdot \delta_{\text{F}} - 4}{2} \quad (21)$$

It is, therefore, absolutely necessary to use the number distribution data if seeking the aspect ratio of a representative particle, as the model is derived to include the mode value. The mode value is the best approximation to describe the most common particle in the system. In Eqs. (5) and (16), the disc diameter  $d$  was used to calculate the aspect ratio and consequently in the whole derivation of Eq. (21). It is, thus, necessary to transform the equivalent spherical diameter (esd) into the platelet diameter  $d$ . A proposed answer to this was given by Jennings and Parslow (1988) and Jennings (1993) in Table 1.

The platelet diameter is a function of the equivalent spherical diameter (esd) and the aspect ratio  $\rho$  as shown in Eq. (22).

$$\rho = \frac{\varepsilon_{\text{BET}} \cdot d_{N50}(\text{esd}_{N50}, \rho) \cdot e^{-\ln^2\left(\frac{\text{esd}_{N84}}{\text{esd}_{N50}}\right)} \cdot \delta_{\text{M}} - 4}{2} \quad (22)$$

This may then be solved by iteration until convergence is achieved.

In the case where the aspect ratio of coarse and fine particles in a sample can differ, the variables  $\text{esd}_{N84}$  and  $\text{esd}_{N50}$  in the exponent would require a modification in respect to the conversion factor expressing the platelet diameter. In the case described here, this information was not known a priori, and thus, a constant aspect ratio throughout the whole particle size distribution was assumed.

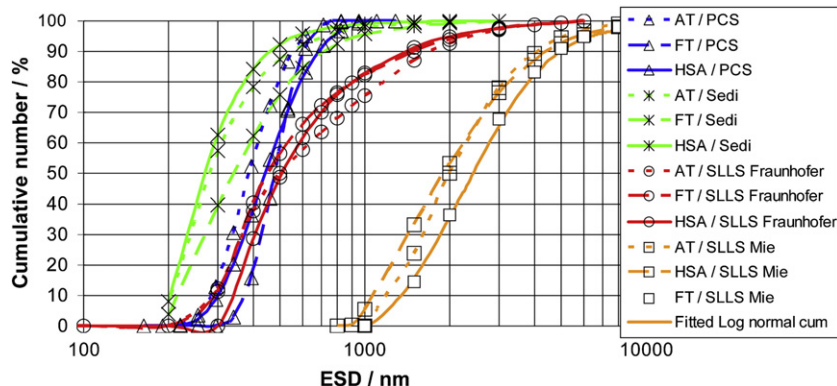


**Fig. 5.** Particle size distribution by photon correlation spectroscopy (PCS), static laser light scattering (SLLS) and sedimentation for the three talc grades (number based).

Furthermore, the definition of an aspect ratio distribution spanning a particle size distribution is a highly complex topic (Pabst and Berthold, 2007) and would not go hand in hand with the intended fast and simple solution.

Thus, all the open questions and incomplete assumptions made by Hohenberger were answered by following the proposed model in this study.

## 2. Materials and methods

### 2.1. The minerals

The Finnish talc (FT) (Fig. 1) was sourced from Mondo Minerals B.V.,<sup>3</sup> available as Finntalc P05. It had a specific surface area determined by nitrogen adsorption of  $9 \text{ m}^2 \text{ g}^{-1}$ .

The Australian talc (AT) (Fig. 2) was sourced from Mondo Minerals B.V., available as Westmin PCS. It had a specific surface area of  $19 \text{ m}^2 \text{ g}^{-1}$ .

The high surface area talc grade (HSA) (Fig. 3) was specially manufactured by comminuting the coarser Finnish talc grade originating from the region of Sotkamo, Finland. It had a specific surface area of  $45 \text{ m}^2 \text{ g}^{-1}$ . XRD analysis of all talc samples similarly indicated talc and associated chlorite.

The sample of Laponite (Fig. 4) was provided by Rockwood additives,<sup>4</sup> available as Laponite® RD. It had a specific surface area of  $330 \text{ m}^2 \text{ g}^{-1}$ . It had the general formula  $\text{Si}_8\text{Mg}_{5.45}\text{Li}_{0.4}\text{H}_4\text{O}_{24}\text{Na}_{0.7}$  (Mourchid et al., 1995).

### 2.2. The methods

#### 2.2.1. XRD

The samples were analysed with a Bruker D8 Advanced powder diffractometer (2.2 kW X-ray tube, a sample holder, a  $\theta$ – $\theta$  goniometer, and a point scintillator, Ni-filtered  $\text{Cu K}\alpha$  radiation). The profiles were chart recorded automatically using a scan speed of  $0.7^\circ$  in  $2\theta$  per minute. The mineral content was estimated by the DIFFRAC<sup>plus</sup> software packages<sup>5</sup> EVA and SEARCH, based on reference patterns of the ICDD PDF 2 database.

#### 2.2.2. Density

The density of the mineral powders was determined with the AccuPyc® 1330 pycnometer from Micromeritics.

#### 2.2.3. Specific surface area

The specific surface area was determined with the Gemini 2360 from Micromeritics. The samples were outgassed at  $250^\circ\text{C}$  for 30 min under nitrogen in a Micromeritics<sup>6</sup> Flow Prep 060.

#### 2.2.4. Sedimentation

The samples were measured on the Sedigraph® 5120 from Micromeritics. All samples were diluted with a 0.1% solution of sodium diphosphate ( $\text{Na}_4\text{P}_2\text{O}_7$ ). Samples of 10 g dry talc were dispersed in  $100 \text{ cm}^3$  of the diphosphate solution with a high speed blender (Polytron<sup>7</sup> PT 3100) for 15 min at  $15,000 \text{ min}^{-1}$  followed by ultrasonication for 10 min in a 130 W ultrasonic bath.

#### 2.2.5. Laser light scattering

A few drops of the dispersions were diluted with a 0.1% solution of sodium diphosphate. The samples were measured with the Malvern Mastersizer 2000. The laser obscuration was set to be between 10 and 20%.

#### 2.2.6. Photon correlation spectroscopy

A few drops of the dispersions were diluted with a 0.1% solution of sodium diphosphate and measured on the Malvern<sup>8</sup> Zetasizer Nano ZS.

## 3. Results and discussion

The specific surface areas of the investigated materials lay between 9 and  $330 \text{ m}^2 \text{ g}^{-1}$  and the density between 2570 and  $2750 \text{ kgm}^{-3}$  (Table 2). The specific surface area of a dispersed product may differ from the one measured by nitrogen adsorption in the dry state. For the investigated model it is crucial to apply the specific surface area of the dispersed particle. This was valid for the talc particles but not for Laponite.

The particle size data obtained by sedimentation suggested the presence of finer particles (Fig. 5). Disc-like particles will not settle like a sphere following the direct and shortest path but rather will float and oscillate like the falling leaves moving also side-ways. The photon correlation spectroscopy data showed a step log-normal distribution (Fig. 5). The static laser light scattering with Fraunhofer optics did not yield a log-normal size distribution and showed an increased amount of coarse material (Fig. 5). Static laser light scattering using the true Mie theory seems only to detect the very coarse fraction of talc particles (Fig. 5).

The  $d_{N50}$  and  $d_{N84}$  values (Table 3) were used to calculate the mode values which were consequently converted into the corresponding aspect ratios (Table 4).

Each particle size method has its optimal size region for analysis and some of the methods are affected more strongly by anisometric shapes than others. These facts also influenced the determination of the aspect ratio. PCS measurements are not so strongly affected by anisometric shapes than are the others (Jennings and Parslow, 1988) since the detection in PCS excludes particles that do not undergo random Brownian motion and, thus, there is no preferred orientation for the particles like in the case of sedimentation. The particle size was already at the upper limit for PCS measurements. The Fraunhofer model is, in theory, only valid for particles with a diameter five times larger than the illuminating wavelength (Schmidt, 2000). Sedimentation by Stokes' law for anisometric disc-like particles is perturbed due to the falling leaf effect, which becomes more and more significant the more the aspect ratio increases, and, thus, the method is not reliable for high aspect ratio particles. Also the other models of Jennings and Parslow (1988) and Pabst and Berthold (2007) depend on the sedimentation result and suffer from the same root problem. However, the opposite was observed for the HSA talc particles. The number based sedimentation particle size data suggested the presence of too coarse particles and thus the resulting aspect ratio was higher than the one calculated by the other methods. The same effect also led to an underestimation of the aspect ratio by the model of Jennings and Parslow (1988) and Pabst and Berthold (2007). Finally, the laser diffraction based on the true Mie theory was overestimating the coarse fraction of the talc samples, although, from a purely physical point of view of equivalent size, interpretation by the Mie theory seems more appropriate. Assumptions like isotropic spheres, for which the Mie theory is valid, may lead to erroneous deconvolution for systems with anisotropic particles (Pabst

<sup>3</sup> Mondo Minerals B.V., Kaijuitweg 8, 1041 AR, Amsterdam, Netherland.

<sup>4</sup> Rockwood Clay Additives GmbH, Stadtwaldstrasse 44, 85368 Moosburg, Germany.

<sup>5</sup> Bruker AXS GmbH, Östliche Rheinbrückenstr. 49, 76187 Karlsruhe, Germany.

<sup>6</sup> Micromeritics NV/SA, Eugene Plaskyalaan 140, 1030 Brussels, Belgium.

<sup>7</sup> Kinematica AG, Luzernerstrasse 147a, CH-6014 Luzern, Switzerland.

<sup>8</sup> Malvern Instruments Ltd., Enigma Business Park, Grovewood Road, Malvern, Worcestershire WR14 1XZ, United Kingdom.

**Table 4**

Calculated aspect ratio for the three talc particles. The aspect ratios were calculated by Eq. (22). In addition the aspect ratios were calculated based on the model of Pabst and Berthold (2007) (Eq. (3)) and on the model of Jennings and Parslow (1988) for oblate spheroids (Eq. (1)) and discs (Eq. (2)). All calculations were based on the mode value from the corresponding  $d_{N50}$  and  $d_{N84}$  values in Table 3.

Model	Method	FT	AT	HSA	Comment
Gantenbein et al. (Eq. (22))	PCS	6	12	37	Upper limit of the particle size range
	SLLS/Fraunhofer	2	8	35	Only log-normal in a certain region
	Sedigraph®	2	11	84	Mass to number transformation
	SLLS/Mie	85	207	590	Over estimating the coarse fraction
Jennings and Parslow for oblate spheroids (Eq. (1))	Sedigraph®/SLLS Fraunhofer	5	5	7	Falling leaf effect
Jennings and Parslow for discs (Eq. (2))	Sedigraph®/SLLS Fraunhofer	6	6	9	Falling leaf effect
Pabst and Berthold (Eq. (3))	Sedigraph®/SLLS Fraunhofer	9	9	12	Falling leaf effect

**Table 5**

Particle disc diameter  $d$  and disc thickness  $t$  in nm.

Method	FT		AT		HSA	
	$d$ /nm	$t$ /nm	$d$ /nm	$t$ /nm	$d$ /nm	$t$ /nm
PCS	660	110	540	45	630	17
SLLS/Fraunhofer	360	150	390	48	600	17
Sedigraph®	260	180	500	45	1390	17
SLLS/Mie	7030	80	8000	39	9600	16

et al., 2000). It is, therefore, suggested to apply either PCS or static laser light scattering with Fraunhofer optics. PCS showed the least number of drawbacks compared to the other methods when considering the whole particle size range investigated in this paper, though the upper size limit of Brownian motion is restrictive. Static laser light scattering with Fraunhofer optics is limited in respect to the fine particle analysis, though in the exemplified cases it did reach the lower limit of the particle size.

The models of Jennings and Parslow (1988) and Pabst and Berthold (2007) could not clearly distinguish the aspect ratios of the different talc particles based on the number based distribution data.

Based on the values calculated above, together with Eq. (5) and the equations in Table 1, the particle dimensions diameter  $d$  and thickness  $t$  were calculated (Table 5).

The different particle size measurement methods indicated similar particle thickness values. The thickness of the low surface area Finnish talc (FT) varied between 80 and 180 nm. The thickness of the Australian talc particles was ~40–50 nm and of the highly delaminated talc particles ~17 nm. The crystallographic defined talc layer is 0.92 nm thick (Bergaya et al., 2006). The thickness mainly controls the specific surface area of the particles, and, thus, the surface area determination is a sensitive method. Of course, for lower surface area materials this influence becomes smaller, and the particle thickness is then also affected by the disc diameter. The disc diameter varied strongly for the different talc grades and measurement methods, mainly as a result of the different responses of the particle size measurement methods. Nevertheless, the results for the FT and AT talc particles with PCS, Fraunhofer and Sedigraph® particle size data gave similar results, whereas the results for the HSA grade were only similar for the PCS and Fraunhofer particle size data.

Besides the calculations quoted above, which were based on the number particle size distribution, it is also possible to use the mass or volume based particle size distribution data (Table 6). Similar particle sizes were only found for the PCS measurements. This is because of the steep distribution of the data in the PCS measurement. Since the PCS measurements are restricted to the Brownian motion limit, they do underestimate the aspect ratio. Similar aspect ratios were calculated for the Finnish and Australian talc particles with the particle size data from the static laser light scattering using Fraunhofer optics and the sedimentation technique. These aspect ratios compare also well with the aspect ratios calculated by the model of Jennings and Parslow (1988) and Pabst and Berthold (2007). In the case of the HSA talc the falling leaf effect for very fine platelets perturbed the aspect ratio values for all models that base on the sedimentation technique. The current model underestimates the aspect ratio, if the particles are too fine whereas the models of Jennings and Parslow (1988) and Pabst and Berthold (2007) overestimate the aspect ratio if the particles are too fine to be measured in the Sedigraph®.

The sedimentation data allowed us to consider the contrast between mass/volume and number probability distribution of particle size. When using mass/volume distribution, the aspect ratios appear much greater, as the distribution mass median is shifted to larger particle size than the number median. The exception to this finding is the HSA talc grade, for which the aspect ratio reduces to 22. This, at first sight unexpected, effect clearly relates to the inappropriate method of sedimentation of highly delaminated platy particles. The falling leaf effect suggests much finer particles than are found in reality. Sedimentation data were also used for the models of Pabst et al. (2000) and Jennings and Parslow (1988). It is, therefore, questionable to use these models for platy particles with large

**Table 6**

Aspect ratio of the three different talc particles based on the various models. The values were obtained by inserting the mode value of the volume or mass based distribution data.

Model	Method	FT	AT	HSA
Gantenbein et al. (Eq. (22))	PCS	7	15	50
	SLLS/Fraunhofer	63	114	330
	SLLS/Mie	345	840	4380
	Sedigraph®	62	108	22
Jennings and Parslow for oblate spheroids (Eq. (1))	Sedigraph®/SLLS Fraunhofer	50	80	2800
Jennings and Parslow for discs (Eq. (2))	Sedigraph®/SLLS Fraunhofer	75	120	4300
Pabst et al. (Eq. (3))	Sedigraph®/SLLS Fraunhofer	78	121	4300

**Table 7**  
Aspect ratio calculated with the original Hohenberger model (Eq. (6)) based on number and volume or mass based distribution data.

Method	FT		AT		HSA	
	Number	Volume	Number	Volume	Number	Volume
PCS	4	4	7	9	22	31
SLLS/Fraunhofer	2	44	8	80	25	230
SLLS/Mie	20	56	37	100	70	300
Sedigraph	1	11	3	11	12	6

diameters and very thin thickness, whereas fine particles undergoing strong Brownian rotation are better suited.

For completeness, also the aspect ratios based on the original Hohenberger equation (Eq. (4)) (Table 7) were also calculated based on number distribution and volume or mass distribution data for comparison.

To illustrate the sensitivity of the specific surface area, dispersions of Laponite particles were studied. They could only be measured by PCS (Fig. 6), due to the nanosized dimensions. The curve showed a log-normal distribution with a  $d_{N50}$  of 13 nm and a  $d_{N84}$  of 17 nm. The resulting aspect ratio was 5.2 (Eq. (22)).

For comparison, we considered the following references (Bonn et al., 1999; Kroon et al., 1996, 1998; Mal et al., 2008; Mouchid et al., 1995; Mouchid and Levitz, 1998; Thompson and Butterworth, 1992). The particle disc diameters were around 20–30 nm and the thickness 1 nm. Thus, the aspect ratio would vary between 20 and 30. These values clearly differed from the value of 5.2 determined in this study. This is related to the inappropriate value of the specific surface area determined by nitrogen adsorption. The surface area exposed by the Laponite particles in water is manifold higher than in dry state due to swelling and delamination of the particles. Thus, the available specific surface area of the dispersed particles was approximated as follows.

Based on Eq. (23), the particle thickness  $t$  was calculated as a function of the aspect ratio  $\rho$  with the  $d_{N50}$  of 13 nm and  $d_{N84}$  of 17 nm (Fig. 7).

$$t = \frac{\tan^{-1}(\rho) \cdot esd_{N50} \cdot e^{-\ln^2\left(\frac{esd_{N84,13}}{esd_{N50}}\right)}}{\rho} \quad (23)$$

The grey area in Fig. 7 marks the layer thickness of 0.88–0.92 nm. The aspect ratio is in the range of 20–21, which, according to the equation for PCS given in Table 1, resulted in a particle diameter  $d$  of ~18.4 nm. The specific surface area will therefore be of the order of 930–970 m<sup>2</sup> g<sup>-1</sup>. Calculating the specific surface area of a disc with

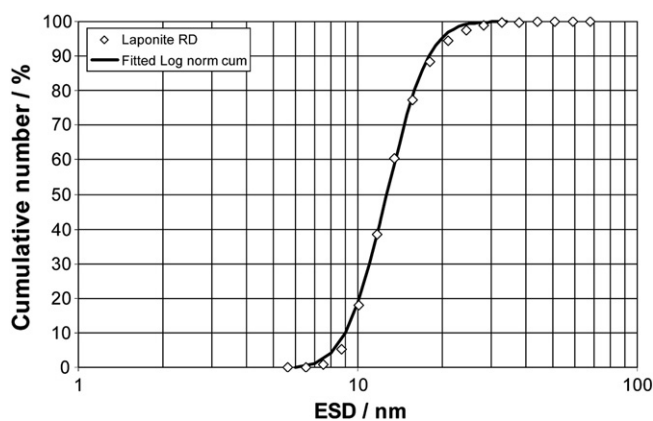


**Fig. 6.** Particle size distribution measured by photon correlation spectroscopy for the Laponite RD.

$d = 18.4$  nm and  $t = 0.9$  nm and a density of 2 570 kgm<sup>-3</sup> results in ~970 m<sup>2</sup> g<sup>-1</sup>.

#### 4. Conclusions

We discussed the equations of Jennings and Parslow (1988) for the application of equivalent spherical diameters and their relation to real particle dimensions. Furthermore, the model of Hohenberger was derived and further developed by clearly defining which parameters have to be inserted for an appropriate use. Practical examples for different talc particles varying in their specific surface area and geological origin were presented, using different particle size determination methods like photon correlation spectroscopy (PCS), static laser light scattering interpreted with different theories (Fraunhofer and Mie) as well as the sedimentation technique. An aspect ratio of ~6 for a Finnish talc (FT) grade with low specific surface area, ~12 for an Australian talc (AT) grade with medium specific surface area and an aspect ratio of ~37 for a Finnish talc grade with high specific surface area (HSA) were found based on PCS particle size data. The results were compared also with other models, which are based on the particle size distribution data as proposed by Pabst and Berthold (2007) and Jennings and Parslow (1988). The use of Laponite clearly revealed a weakness of the presented model. The specific surface area determined in the dry state by nitrogen adsorption is for some minerals not representing the geometrically defined exterior available surface area in water. However, this drawback was shown to be an opportunity to approximate the total specific surface area of the delaminated Laponite particles, which in the current study was determined to be 930–970 m<sup>2</sup> g<sup>-1</sup>.

Based on the aspect ratios derived by adopting the presented model, the particle diameter  $d$  and thickness  $t$  were calculated. Despite the sometimes different responses for the diameter  $d$ , comparable values for the particle thickness  $t$  were found. This is not surprising. According to the assumed model, the particle thickness mainly determines the specific surface area. The average particle thicknesses lay for the low surface area Finnish talc (FT) between 80 and 180 nm, for the medium surface area Australian talc (AT) between 40 and 50 nm and was for the highly exfoliated Finnish talc (HSA) around 17 nm.

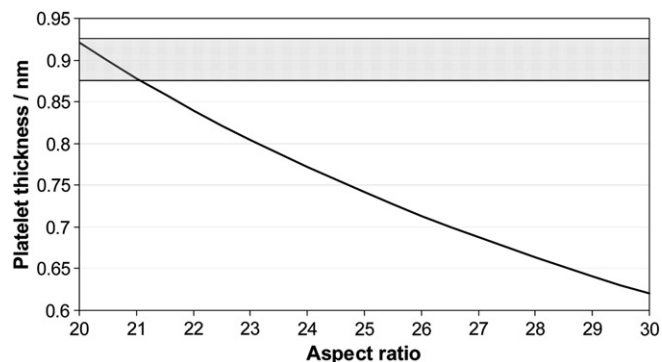


**Fig. 7.** Platelet thickness of Laponite RD calculated with Eq. (23) and with the  $d_{N50} = 13$  nm and  $d_{N84} = 17$  nm.

The particle size measurement method has to be chosen carefully. The method should be applicable over the relevant size range of the particles in question and it should not be affected by the anisotropy of the particles, such as the falling leaf analogy observed for the sedimentation technique. For the talc and Laponite particles tested in this study, photon correlation spectroscopy is suggested as preferable. If not available or not relevant in respect to the particle size (considering materials larger than 100 nm diameter) static laser light scattering with Fraunhofer optics can be used.

## References

- Aitchison, J., Brown, J.A.C., 1957. The Lognormal Distribution. Cambridge University Press, Cambridge UK.
- Allen, T.A., 1997. Particle Size Measurement, fifth ed. Chapman & Hall, London.
- Aris, R., 1957. On shape factors for irregular particles—I. The steady-state problem. Diffusion and reaction. Chem. Eng. Sci. 6, 262–268.
- Baudet, G., Bizi, M., Rona, J.P., 1993. Estimation of the average aspects ratio of lamellae-shaped particles by laser diffractometry. Part. Sci. Technol. 11, 73–96.
- Bergaya, F., Theng, B.K.G., Lagaly, G., 2006. Handbook of Clay Science, Volume 1. Elsevier, Amsterdam.
- Bonn, D., Kella, H., Tanaka, H., Wegdam, G., Meunier, J., 1999. Laponite: what is the difference between a gel and a glass? Langmuir 15, 7534–7536.
- Brunauer, S., Emmett, P.H., Teller, E., 1938. Adsorption of gases in multimolecular layers. J. Am. Chem. Soc. 60, 309–319.
- Casal, J., Lucas, A., Arnaldos, J., 1985. A new method for the determination of shape factor and particle density. Chem. Eng. J. 30, 155–158.
- Champion, J.V., Downer, D., Meeten, G.H., Gate, L.F., 1978. Magnetic and optical properties of kaolinite particles in aqueous dispersion. J. Chem. Soc., Faraday Trans. 2 (74), 843–863.
- Champion, J.V., Meeten, G.H., Moon, B.R., Gate, L.F., 1979. Optical extinction of randomly orientated and shear flow orientated colloidal kaolinite particles. J. Chem. Soc., Faraday Trans. 2 (75), 780–789.
- Conley, R.F., 1966. Statistical distribution patterns of particle size and shape in the Georgia kaolins. Clay Miner. 14, 317–330.
- Ferrage, E., Martin, F., Petit, S., Pejo-Soucaille, S., Micoud, P., Fourty, G., Ferret, J., Salvi, S., De Parseval, P., Fortune, J.P., 2003. Evaluation of talc morphology using FTIR and H/D substitution. Clay Miner. 48, 141–150.
- Gane, P.A.C., Coggon, L., 1987. Blade geometry: its effect on coating colour dynamics and coated sheet properties. Tappi J. 70, 87–96.
- Gane, P.A.C., Watters, P., 1989. Pigment particle orientation: an analysis of the opportunities for optimising blade coater runnability and coated sheet properties by controlled flow geometry. Pap. Tim. 5, 517–533.
- Gane, P.A.C., Hooper, J.J., Grunewald, A., 1995. Coating pigment orientation: a comparative analysis of the application mechanisms and properties of blade and roll coatings, Tappi Coating Conference. Tappi Press, Dallas, Atlanta.
- Gane, P.A.C., 1997. Relaxation-induced dilatancy in separable visco-elastic suspensions: proposing a novel rheological phenomenon. Tappi Advanced Coating Fundamentals Symposium. Tappi Press, Philadelphia, Atlanta.
- Gane, P.A.C., Burri, P., Spielmann, D.C., Drechsel, J., Reimers, O., 1997. Formulation optimisation for improved runnability of high speed pigmented coatings on the metered size press. Tappi Coating Conference. Tappi Press, Philadelphia, Atlanta.
- Gane, P.A.C., 2001. Mineral pigments for paper: structure, function and development potential (Part I). Wochenbl. Papierfabr. 129, 110–116.
- Gantenbein, D., Schoelkopf, J., Matthews, G.P., Gane, P.A.C., in press. Determining the size distribution-defined aspect ratio of rod-like particles. Appl. Clay Sci. doi:10.1016/j.clay.2011.04.020.
- Groszek, A.J., Partyka, S., 1993. Measurements of hydrophobic and hydrophilic surface sites by flow microcalorimetry. Langmuir 9, 2721–2725.
- Hohenberger, W., 2001. Fillers and reinforcements. In: Zwiefel, H. (Ed.), Plastics Additives Handbook. Hanser Publishers, Munich, pp. 901–948.
- Jennings, B.R., 1993. Size and thickness measurement of polydisperse clay samples. Clay Min. 28, 485–494.
- Jennings, B.R., Parslow, K., 1988. Particle size measurements: the equivalent spherical diameter. P. Roy. Soc. A Math. Phys. 419, 139–149.
- Kroon, M., Vos, W.L., Wegdam, G.H., 1998. Structure and formation of a gel of colloidal disks. Phys. Rev. E 57, 1962–1970.
- Kroon, M., Wegdam, G.H., Sprik, R., 1996. Dynamic light scattering studies on the sol-gel transition of a suspension of anisotropic colloidal particles. Phys. Rev. E 54, 6541–6550.
- Li, Z., Yang, J., Xu, X., Xu, X., Yu, W., Yue, X., Sun, C., 2002. Particle shape characterization of fluidized catalytic cracking catalyst powders using the mean value and distribution of shape factors. Adv. Powder Technol. 13, 249–263.
- Lohmander, S., 2000. Aspect ratios of pigment particles determined by different methods. Nord. Pulp Paper Res. J. 15, 221–230.
- Mal, D., Sinha, S., Middy, T.R., Tarafdar, S., 2008. Desiccation crack patterns in drying laponite gel formed in an electrostatic field. Appl. Clay Sci. 39, 106–111.
- Mie, G., 1908. Beiträge zur Optik trüber Medien, speziell kolloidaler Metallösungen. Ann. Phys. 25, 377–445.
- Morris, H.H., Sennett, P., Drexel, R.J., 1965. Delaminated clays—physical properties and paper coating properties. Tappi 48, 92–99.
- Mourchid, A., Delville, A., Lambard, J., Lécolier, E., Levitz, P., 1995. Phase diagram of colloidal dispersions of anisotropic charged particles: equilibrium properties, structure, and rheology of laponite suspensions. Langmuir 11, 1942–1950.
- Mourchid, A., Levitz, P., 1998. Long-term gelation of laponite aqueous dispersions. Phys. Rev. E 57, 4887–4890.
- Murray, H.H., Kogel, J.E., 2005. Engineered clay products for the paper industry. Appl. Clay Sci. 29, 199–206.
- Naito, M., Hayakawa, O., Nakahira, K., Mori, H., Tsubaki, J., 1998. Effect of particle shape on the particle size distribution measured with commercial equipment. Powder Technol. 100, 52–60.
- Pabst, W., Kunes, K., Havrda, J., Gregorova, E., 2000. A note on particle size analyses of kaolins and clays. J. Eur. Ceram. Soc. 20, 1429–1437.
- Pabst, W., Kunes, K., Gregorova, E., Havrda, J., 2001. Extraction of shape information from particle size measurements. Br. Ceram. T. 100, 106–109.
- Pabst, W., Berthold, Ch., Gregorova, E., 2006a. Size and shape characterization of polydisperse short-fiber systems. J. Eur. Ceram. Soc. 26, 1121–1130.
- Pabst, W., Gregorova, E., Berthold, Ch., 2006b. Particle shape and suspension rheology of short-fiber systems. J. Eur. Ceram. Soc. 26, 149–160.
- Pabst, W., Berthold, Ch., 2007. A simple approximate formula for the aspect ratio of oblate particles. Part. Part. Syst. Char. 24, 458–463.
- Pabst, W., Berthold, Ch., Gregorova, E., 2007. Size and shape characterization of oblate and prolate particles. J. Eur. Ceram. Soc. 27, 1759–1762.
- Papirer, E., Balard, H., Jagiello, J., Baeza, R., Claus, F., 1992. Modification and surface characterization of talc. Chemically modified surfaces. Proceedings of the Fourth Symposium on Chemically Modified Surfaces, Chadds Ford, PA, USA.
- Podczek, F., 1997. A shape factor to assess the shape of particles using image analysis. Powder Technol. 93, 47–53.
- Randall, M.G., 1989. Particle Packing Characteristics. Metal Powder Industries, New Jersey.
- Scherrer, P., 1918. Bestimmung der Größe und der inneren Struktur von Kolloidteilchen mittels Röntgenstrahlen, 26. Nachr. Ges. Wiss., Göttingen, pp. 98–100.
- Schmidt, W., 2000. Optische Spektroskopie—Eine Einführung, 2. Auflage. Wiley-VCH, Weinheim.
- Schoelkopf, J., Gantenbein, D., Dukhin, A.S., Goetz, J.P., Gane, P.A.C., 2008. Novel particle size characterization of coating pigments: comparing acoustic spectroscopy with laser light scattering and sedimentation techniques. Advanced Coating Fundamentals Symposium, Montreal, Canada.
- Slepety, R.A., Cleland, A.J., 1993. Determination of shape of kaolin pigment particles. Clay Min. 28, 495–508.
- Thompson, D.W., Butterworth, J.T., 1992. The nature of Laponite and its aqueous dispersions. J. Colloid Interface Sci. 151, 236–243.
- Yekeler, M., Ulusoy, U., Hicyilmaz, C., 2004. Effect of particle shape and roughness of talc mineral ground by different mills on the wettability and floatability. Powder Technol. 140, 68–78.
- Yildirim, I., 2001. Surface free energy characterization of powders. Ph.D. Thesis, Virginia Polytechnic Institute and State University, Blacksburg, Virginia.